

## **Electronic Supplementary Information**

### **Multi-band Photon avalanche controlling performance of BiOCl:**

### **Er<sup>3+</sup> crystals through facilely Yb<sup>3+</sup> doping**

Yongjin Li<sup>1,2</sup>, Zhiguo Song<sup>1\*</sup>, Ronghua Wan<sup>1</sup>, Qun Liu<sup>1</sup>, Yuting Zhou<sup>1</sup>, Jianbei Qiu<sup>1\*</sup>,

Zhengwen, Yang<sup>1</sup>, Zhaoyi Yin<sup>1</sup>

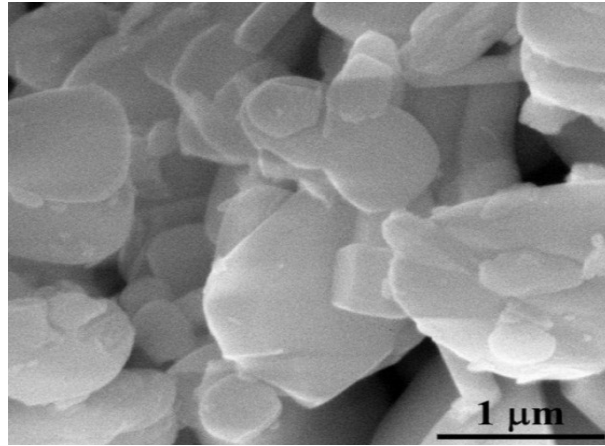
<sup>1</sup> *School of Materials Science and Engineering, Kunming University of Science and*

*Technology, Kunming, 650093, China*

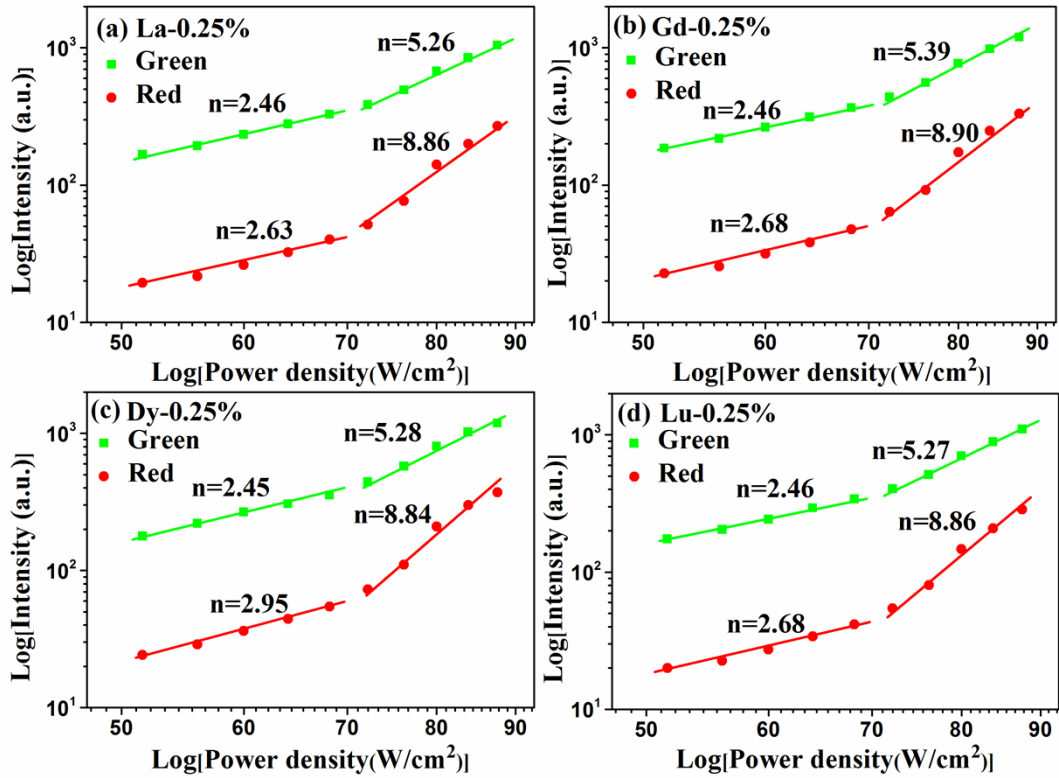
<sup>2</sup> *Department of Science Research, Yunnan Technology and Business University,*

*Kunming, 651700, China*

\* Corresponding Author: E-mail: [songzg@kmust.edu.cn](mailto:songzg@kmust.edu.cn)

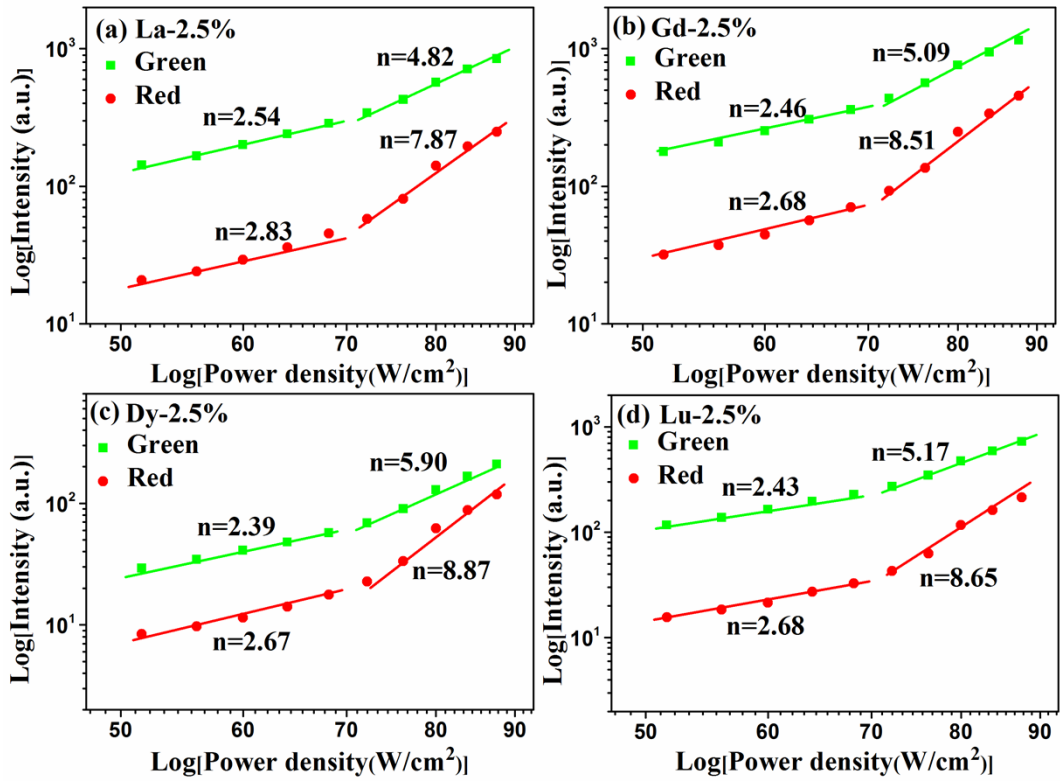


**Fig. S1.** SEM patterns of  $\text{Bi}_{0.9725}\text{Er}_{0.0025}\text{Yb}_{0.025}\text{OCl}$  crystals.

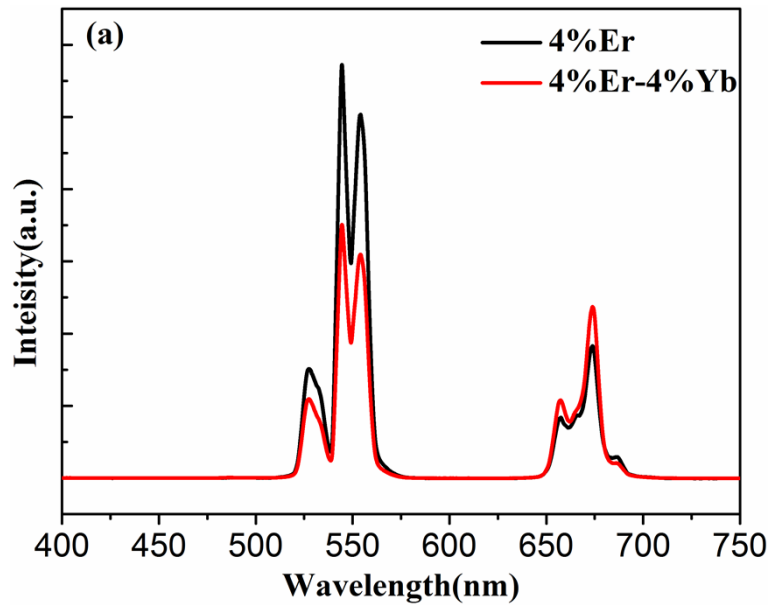


**Fig. S2.** Power dependence of UC intensities of  $\text{Bi}_{0.995}\text{Er}_{0.0025}\text{Re}_{0.0025}\text{OCl}$  crystals. (Re

= La, Gd, Dy and Lu)



**Fig. S3.** Power dependence of UC intensities of Bi<sub>0.9725</sub>Er<sub>0.0025</sub>Re<sub>0.025</sub>OCl crystals. (Re = La, Gd, Dy and Lu)



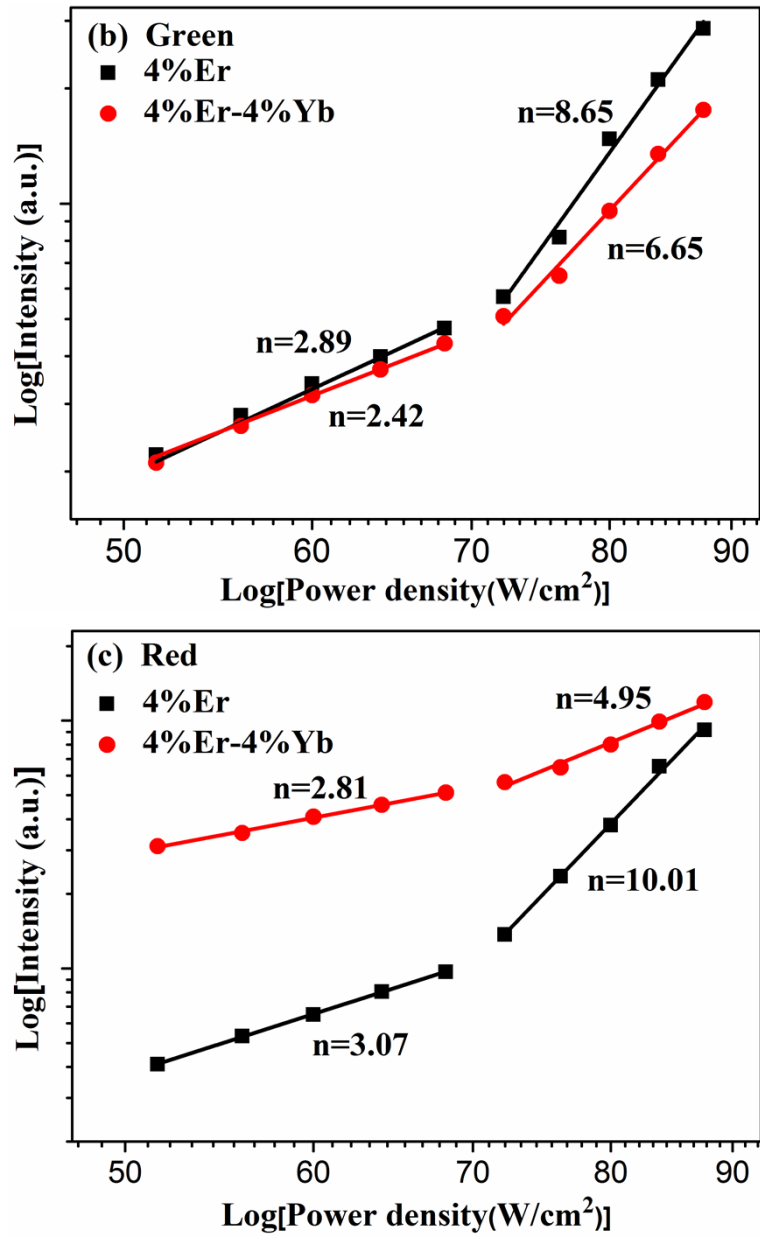


**Fig. S4** (a) UC spectra of 4% Er<sup>3+</sup> doped and 4% Er<sup>3+</sup>-4%Yb<sup>3+</sup> coped BiOBr crystals; Pump power dependence of UC emission of (b) green (c) red emission.

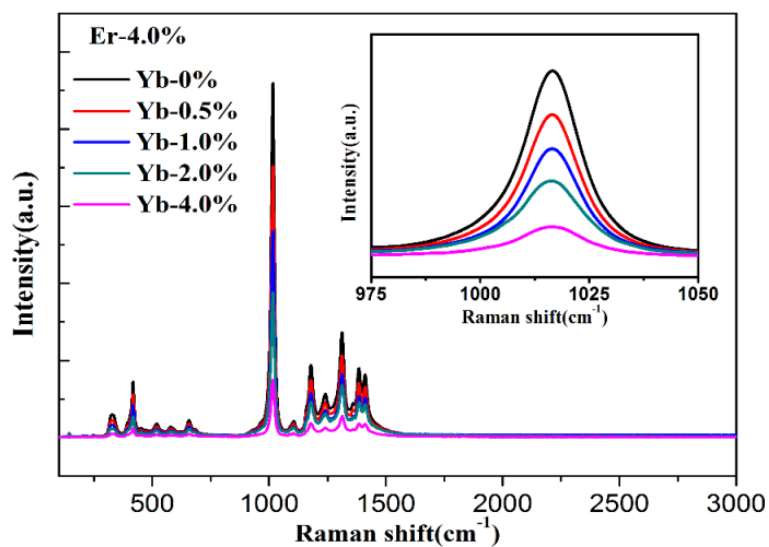


**Fig. S5.** Raman spectra of  $\text{Bi}_{(1-0.04-y)}\text{Er}_{0.04}\text{Yb}_y\text{OCl}$  crystals with different  $\text{Yb}^{3+}$  concentration. The inset is the enlarged Raman spectra of the peak at  $1015\text{ cm}^{-1}$ .

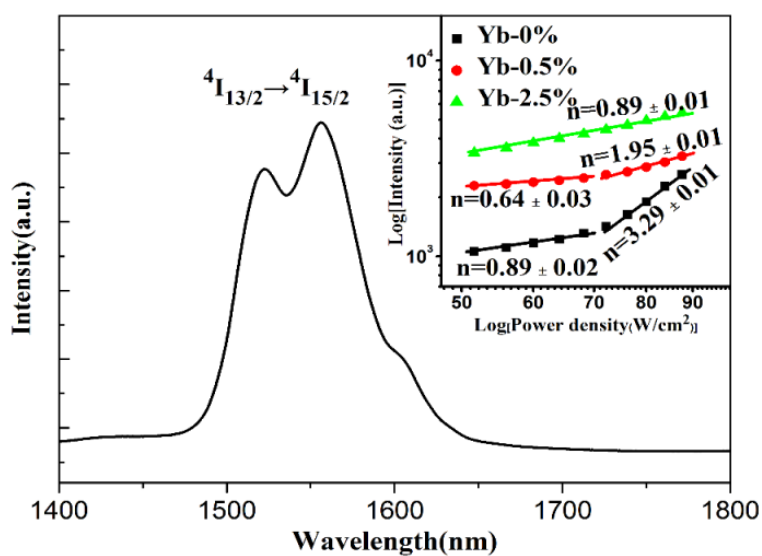


**Fig. S6.** NIR fluorescent spectra of  $\text{Bi}_{0.9725}\text{Er}_{0.0025}\text{Yb}_{0.025}\text{OCl}$  crystals under excitation at  $980\text{ nm}$ . The inset is the power dependence of the NIR emission ( $1550\text{ nm}$ ) with different  $\text{Yb}^{3+}$  concentrations.

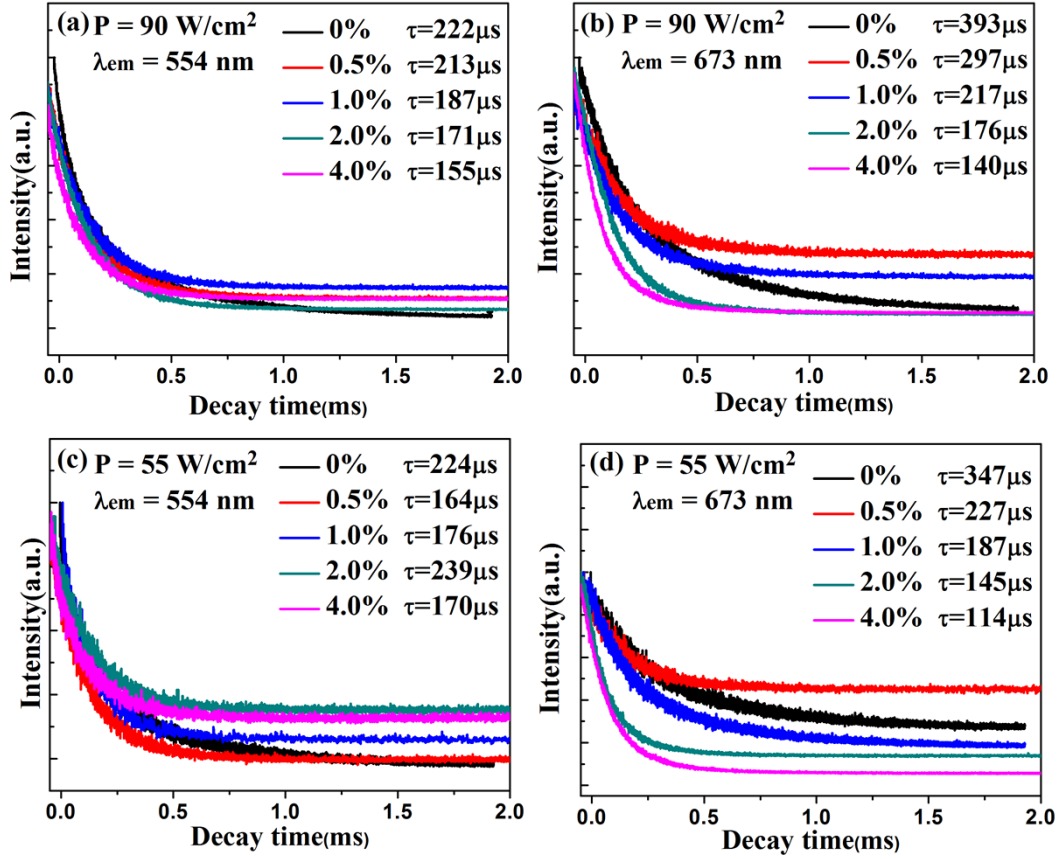


**Fig. S7.** UC emission lifetime decay curves of  $\text{Bi}_{(1-0.04-y)}\text{Er}_{0.04}\text{Yb}_y\text{OCl}$  crystals with various  $\text{Yb}^{3+}$  concentration under excitation at 980 nm with power density of 90  $\text{W/cm}^2$  (upon threshold) and 55  $\text{W/cm}^2$  (below threshold). (a)  $^4\text{S}_{3/2}$  level and (b)  $^4\text{F}_{9/2}$  level upon threshold; (c)  $^4\text{S}_{3/2}$  level and (d)  $^4\text{F}_{9/2}$  level below threshold point.

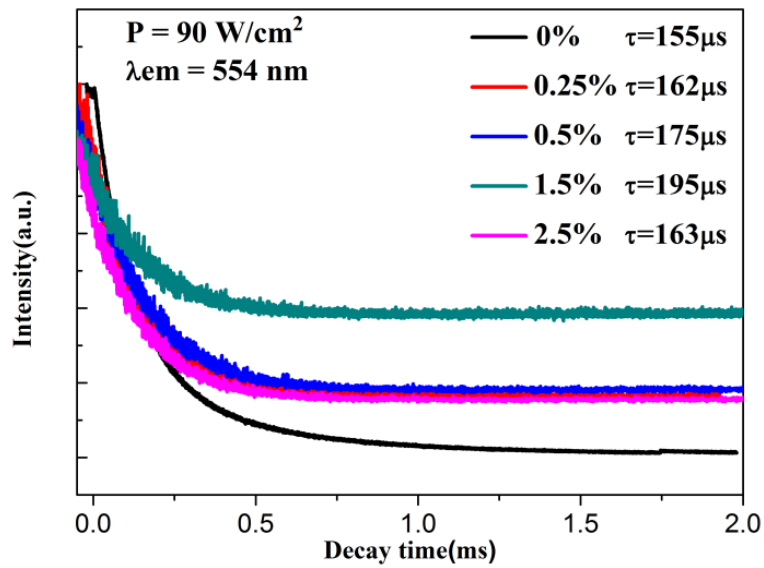


**Fig. S8.** UC emission lifetime decay curves of  $^4\text{S}_{3/2}$  level of  $\text{Bi}_{(1-0.025-x)}\text{Er}_{0.025}\text{Yb}_x\text{OCl}$

crystals with various Yb<sup>3+</sup> concentration under excitation at 980 nm with power density of 90 W/cm<sup>2</sup> (upon threshold).

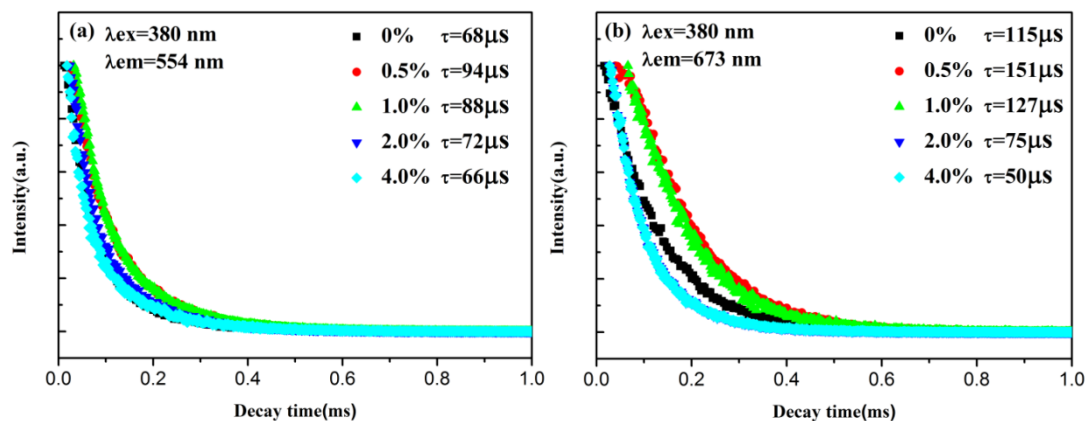


**Fig. S9.** The downshifting luminescence lifetime decay curves of (a) <sup>4</sup>S<sub>3/2</sub> and (b) <sup>4</sup>F<sub>9/2</sub> level of Bi<sub>(1-0.04-y)</sub>Er<sub>0.04</sub>Yb<sub>y</sub>OCl crystals with various Yb<sup>3+</sup> concentration under 380 nm excitation.

The UC and downshifted luminescence lifetimes were both fitted using a single exponential function.

$$I(t) = I_0 + A_1 \exp(-t/\tau_1)$$

where  $I$  and  $I_0$  are the luminescence intensity at time  $t$  and 0,  $A_1$  is a constant,  $t$  is the time, and  $\tau_1$  is the decay time for the exponential components, respectively. In the case of UC emission process (Fig.S5), the lifetimes of samples upon excitation threshold point is just slightly longer than those below threshold point, which is probably due to the influence of increasing power on the enhancement of ET UC process.<sup>1,2</sup> Meanwhile, the elevated amount of Yb<sup>3+</sup> dopants concentration decrease the lifetimes of green and red light upconverted levels, exhibiting the similar effect on the lifetime of conventional UC emissions,<sup>3,4</sup> in which Yb<sup>3+</sup> ions may act as trapping

centers and dissipate energy nonradiatively.<sup>5</sup> It is necessary to clarify that the decrease of lifetimes should not be the critical factors restraining the PA behaviors. For instance, for the samples with 0.25 % mol Er<sup>3+</sup> ions, the lifetimes of green UC emission level increase first and then decrease with increase in the Yb<sup>3+</sup> dopant upon threshold (Fig. S6, Supporting Information).

In the case of downshifting Stocks process, the lifetimes of green and red emission levels excited by UV light (380 nm) increase at first and decrease with increasing Yb<sup>3+</sup> dopants subsequently (Fig. S7). The most likely cause of this trend is that Yb<sup>3+</sup> dopants can weaken the magnitude of lattice vibrations due to Er<sup>3+</sup> doping, which reduce the NVR and prolong the lifetimes of emission levels consequently. On the other hand, the higher concentration Yb<sup>3+</sup> dopant will also act as trapping centers and dissipate energy nonradiatively, and eventually decrease the lifetimes as do in the conventional UC process.<sup>5</sup>

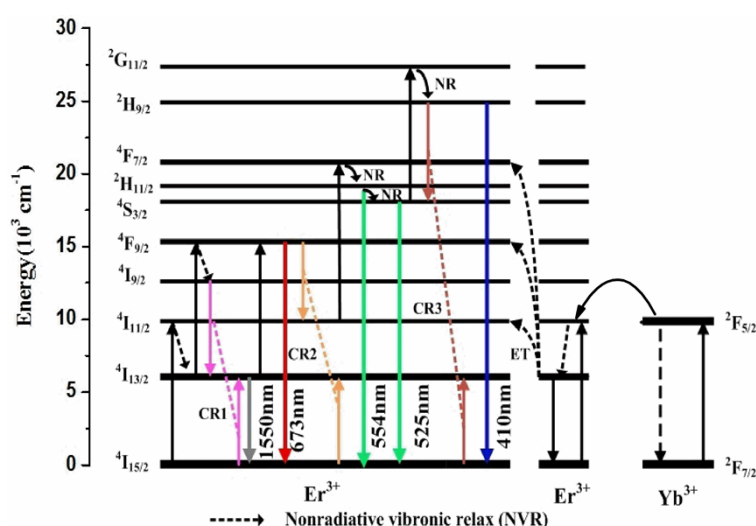


**Fig. S10** Energy levels diagram of Er<sup>3+</sup> and Yb<sup>3+</sup> and possibly PA UC mechanisms

Fig. S10 depicts energy levels of Er<sup>3+</sup> and Yb<sup>3+</sup> ions as well as the proposed mechanism of PA responsible for violet, green, red and NIR emissions. For the PA process, it is generally



based on the existence of an efficient cross-relaxation (CR) process which can populate the intermediate state. We supposed that the  $^4I_{13/2}$  level will become a dominant reservoir level through relaxation from  $^4I_{11/2}$  level under the effect of intense internal polarized electric field as well as intense nonradiative vibration relaxation that is originated from the vibration of lattice and surface absorbed groups. The great enhancement of electron phonon interaction upon the threshold of excitation power can readily remedy the energy mismatch between the transitions with the intermediate energy level of  $Er^{3+}$  ion. Thus, the intermediate population of  $^4F_{9/2}$  level (red emission),  $^2H_{11/2}/^4S_{3/2}$  level (green emission) and  $^2H_{9/2}$  level (violet emission) could be greatly enhanced and resulted in the occurrence of remarkable ratio between the population of reservoir level and the excited-state level, which initiated necessary condition for the UC PA processes and lead to the NIR PA behavior synchronously. However, the increase of  $Yb^{3+}$  ion dopant concentration reduced the magnitude of internal polarized electric field and polarizable chemical environment of BiOCl crystals, which would reduce the excitation and transition of  $Er^{3+}$  ions, resulting in the decrease of the cycle numbers for the CR processes of UC and NIR PA emissions. Meanwhile, the enhanced ET process from the  $Yb^{3+}$  to  $Er^{3+}$  ions simultaneously improve the population of upconverting levels through the traditional ET processes in most Er-Yb co-doped compounds, thus, the PA phenomenon disappeared consequently.

#### **References:**

1. Y. Li, Z. Song, C. Li, R. Wan, J. Qiu, Z. Yang, Z. Yin, Y. Yang, D. Zhou and Q. Wang,

*Appl. Phys. Lett.*, 2013, **103**, 231104.

2. A. K. Singh, K. Kumar, A. C. Pandey, O. Parkash, S. B. Rai and D. Kumar, *Appl. Phys. B*, 2011, **104**, 1035-1041.
3. P. Du, Z. Xia and L. Liao, *J. Lumin.* 2013, **133**, 226-229.
4. J. Shan, M. Uddi, N. Yao and Y. Ju, *Adv. Funct. Mater.* 2010, **20**, 3530-3537.
5. F. Vetrone, J. Boyer, J. A. Capobianco, A. Speghini, and M. Bettinelli, *J. Appl. Phys.* 2004, **96**, 661-667.